Multilayer Effects on Microstrip Antennas for Their Integration With Mechanical Structures

Chisang You, Manos M. Tentzeris, *Senior Member, IEEE*, and Woonbong Hwang

***Abstract*—The effect of multilayer geometry on microstrip antennas is investigated for the design of antenna-integrated mechanical structure. Changes in the gain of antenna due to the geometry have been determined using a transmission line analogy. Design of high-gain antenna in bandwidth is proposed away from structural resonance. Experiments are done on microstrip antennas covered by superstrates in order to verify high-gain conditions theoretically derived herein. The off-resonant conditions that use practical materials of moderate thickness make it possible to design the antenna-integrated mechanical structure with the perfect integration of high mechanical and electrical performances.**

***Index Terms*—Composite structure, embedded antenna, gain enhancement, integrated antenna, mechanical structure.**

I. Introduction

In THE LAST TEN years, research has been undertaken on the embedding of antennas in load-bearing structural surfaces of aircraft to improve both structural efficiency and antenna performance (Fig. 1) [1]–[3]. Structure, material and antenna designers have joined forces to develop this new high payoff technology called conformal load-bearing antenna structure (CLAS) [3]. Innovative integration of antenna elements should significantly improve the reception quality and manufacturability of vehicles [4]. In order to design the load-bearing antenna structure, we have proposed antenna-integrated composite structure as shown in Fig. 2 [5]–[7].

In [5], [6], the antenna-integrated composite structure was designed using the structural optimization and we reported that high gain was obtained by the structural resonance. To overcome low gain of microstrip antenna, a gain enhancement method relying on structural resonance has been proposed and discussed [8]–[12]. This method involves the addition of a superstrate layer over the substrate. It is referred to as the resonance gain method. By choosing the thicknesses of the substrate and the superstrate layers, a very large gain can be realized. For the practical application, the resonance gain method has been studied using moment method [10]. This resonance gain method involves a limited structural geometry, resonant frequency drift, narrow impedance bandwidth and does not provide a design guide for wide bandwidth.

Manuscript received August 4, 2006; revised November 28, 2006.

C. You and M. M. Tentzeris are with the School of Electrical and Computer Engineering, Georgia Institute of Technology, Atlanta, GA 30308 USA (e-mail: chees@ece.gatech.edu).

W. Hwang is with the Department of Mechanical Engineering, Pohang University of Science and Technology, Pohang, 790-784 South Korea.

Digital Object Identifier 10.1109/TAP.2007.893401

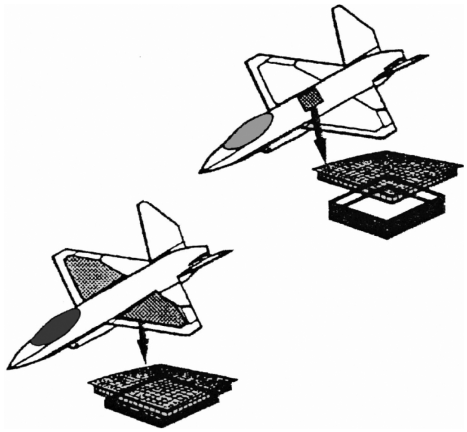

Fig. 1. Antenna in load-bearing structural surface.

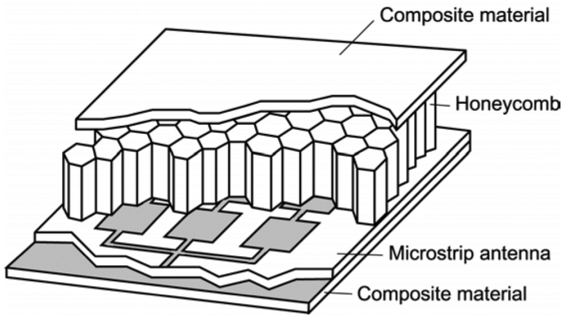

Fig. 2. Microstrip antenna embedded in composite structure.

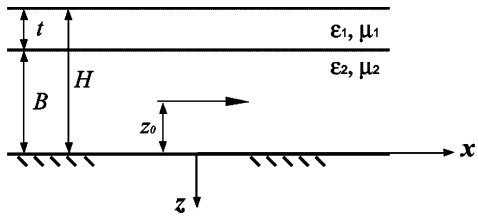

Fig. 3. Superstrate-substrate geometry for theoretical investigation.

In [11], [12], it was suggested that the resonant condition can always be satisfied by adjusting the superstrate position and the value of the resonant gain is a function of the thickness of the superstrate. However, all high-gain conditions obtained by geometrical optimization are not the result of the structural resonance. So far, no research has ever looked at the multilayer effects on microstrip antennas away from the structural resonance.

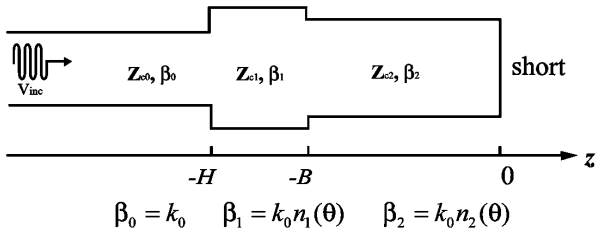

For V_ϕ	For V_θ
$Z_{c0} = \eta_0 \sec\theta$	$Z_{c0} = \eta_0 \cos\theta$
$Z_{c1} = \eta_0 \mu_1 / n_1(\theta)$	$Z_{c1} = \eta_0 n_1(\theta)/\varepsilon_1$
$Z_{c2} = \eta_0 \mu_2 / n_2(\theta)$	$Z_{c2} = \eta_0 n_2(\theta)/\varepsilon_2$

$$n_1(\theta) = \sqrt{n_1^2 - \sin^2\theta} \quad , \quad n_2(\theta) = \sqrt{n_2^2 - \sin^2\theta}$$

Fig. 4. Transmission line analogy of superstrate-substrate geometry.

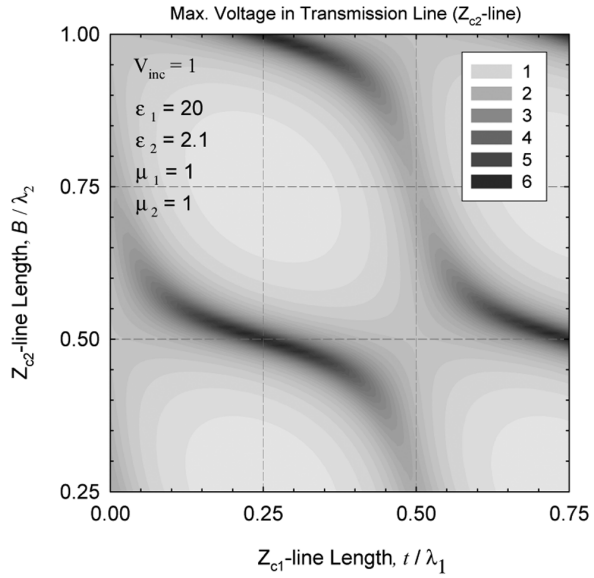

Fig. 5. Maximum voltage strength in transmission line with the change of lengths, t and B.

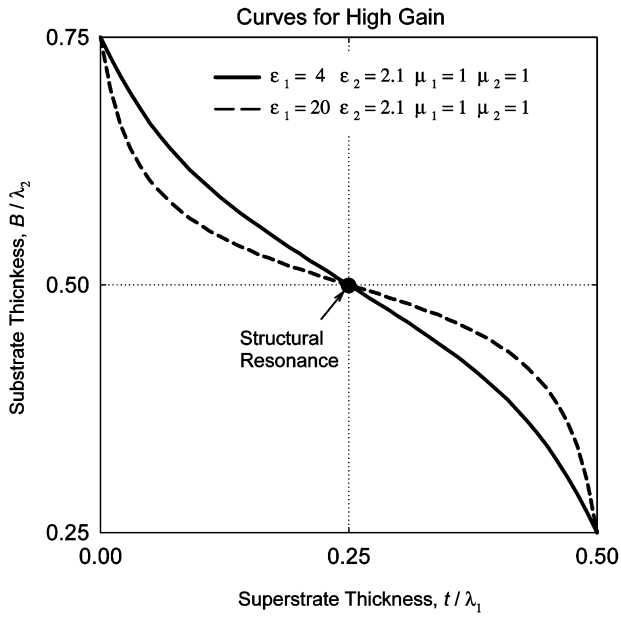

Fig. 6. High-gain curves by superstrate-substrate thicknesses, t and B.

In this paper, the multilayer effects on microstrip antennas are investigated for their integration with mechanical structure. Superstrate-substrate geometry is theoretically analyzed using a transmission line analogy. Experiments are done on microstrip antennas covered by superstrates and compared with the theoretical data.

II. Superstrate-Substrate Geometry

The antenna-integrated composite structure is previously introduced in Fig. 2. Since the change of antenna performances depends on the superstrate (outer composite material), the upper part from the antenna is considered. The theoretical model is a dipole-embedded substrate with the addition of a superstrate over the substrate, as shown in Fig. 3 [8]. The electric dipole is embedded within a grounded substrate of thickness B with relative permittivity and permeability ε_2, μ_2. On top of the substrate is a superstrate layer of thickness t with relative permittivity and permeability ε_1, μ_1. Above the top substrate is free space, with total permittivity and permeability ε_0, μ_0. In this theoretical investigation, material loss is not considered since the degradation in gain in the two-layer structure is very acceptable with a reasonable material loss [12].

A convenient way to analyze the strength of radiation from this antenna structure is by transmission line analogy [8]–[10]. By reciprocity, the E_θ and E_ϕ fields at a point $P(\theta, \phi)$ are the same as the E field at the dipole, due to an infinitesimal dipole source at P, in the θ and ϕ direction. The E field near the layered structure due to this reciprocity source is essentially a plane wave, and hence can be accounted for by modeling each layer as a transmission line [8]. The E_θ field corresponds to an E field from the reciprocity source in the plane of incidence, while the E_ϕ field corresponds to an incident E field normal to the plane of incidence. The following field expressions can be written in spherical coordinates:

$$E_\theta = -\cos\phi\cos\theta \left(\frac{jw\mu_o}{4\pi R}\right) e^{-jk_0 R} V_\theta(\theta) \tag{1}$$

$$E_\phi = \sin\phi \left(\frac{jw\mu_o}{4\pi R}\right) e^{-jk_0 R} V_\phi(\theta) \tag{2}$$

where the functions $V_\phi(\theta)$ and $V_\theta(\theta)$ represent the voltages at $z = -z_0$ in transmission line analogy in Fig. 4. From (1) and

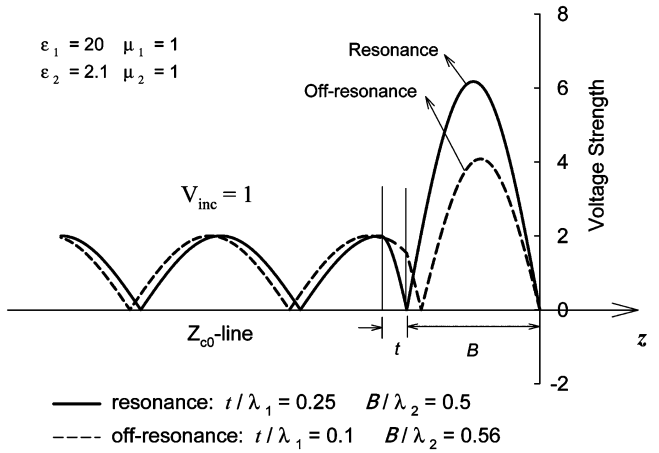

Fig. 7. Voltage in transmission line at resonance and off-resonance.

(2) the gain at angles (θ, ϕ) referred to an isotropic radiator can be expressed as

$$\text{gain}(\theta,\phi) = \frac{4\left(\sin^2\phi|V_\phi(\theta)|^2 + \cos^2\phi\cos^2\theta|V_\theta(\theta)|^2\right)}{\int_0^{\pi/2}(\sin\theta)\left[|V_\phi(\theta)|^2 + \cos^2\theta|V_\phi(\theta)|^2\right]d\theta}. \tag{3}$$

The voltages in the line are the results of multiple reflections at the junctions by a normally incident wave; they depend on Z_{c1}- and Z_{c2}-line lengths, t and B, characteristic impedances, Z_{c1} and Z_{c2}, and propagation constants, β_1 and β_2. The voltage in the Z_{c0} line by an incident wave of strength 1 can then be written as

$$V^{(0)} = e^{-j\beta_0 z} + \Gamma_t e^{+j\beta_0 Z} \text{ in } Z_{c0} \text{ line} \tag{4}$$

where Γ_t is a total reflection coefficient of an incident wave at $z = -H$, which is the sum of partial reflections resulting from two more junctions at $z = 0$ and $-B$. Within the Z_{c1} and Z_{c2} lines, waves bounce back and forth between the two bounding junctions, some penetrating into the other coupling lines. The total voltages on the Z_{c1} and Z_{c2} lines, respectively are the sum of the total traveling wave in $+z$-direction and the wave in $-z$-direction. Therefore

$$V^{(1)} = V_1^+ e^{-j\beta_1 z} + V_1^- e^{+j\beta_1 Z} \text{ in } Z_{c1} \text{ line} \tag{5}$$

and

$$V^{(2)} = V_1^+ e^{-j\beta_2 z} + V_2^- e^{+j\beta_2 Z} \text{ in } Z_{c2} \text{ line} \tag{6}$$

where V_i^+ and $V_i^-(i = 1, 2)$ are the magnitude of the total traveling wave in $+z$- and $-z$-direction, respectively.

The variation of maximum voltage strength in the transmission line (Z_{c2} line) is shown in Fig. 5 with the parametric change of lengths, t and B. The maximum values, being at the centers

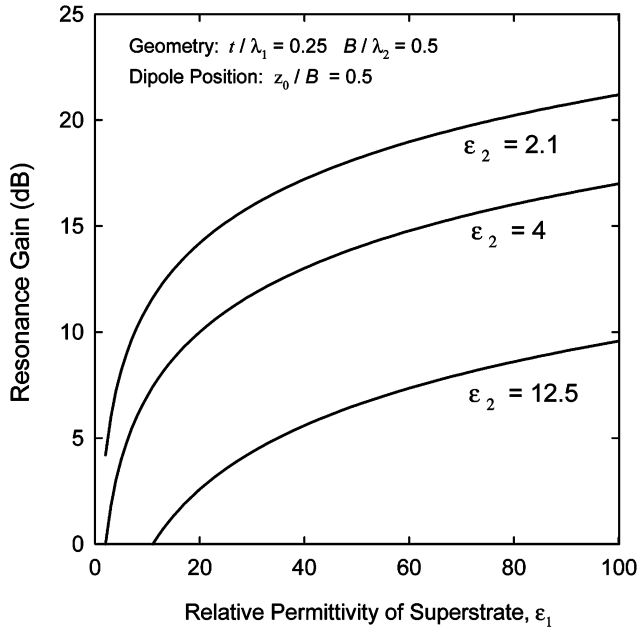

Fig. 8. Resonance gain versus ε_1 of superstrate-substrate geometry ($\mu_1 = \mu_2 = 1$).

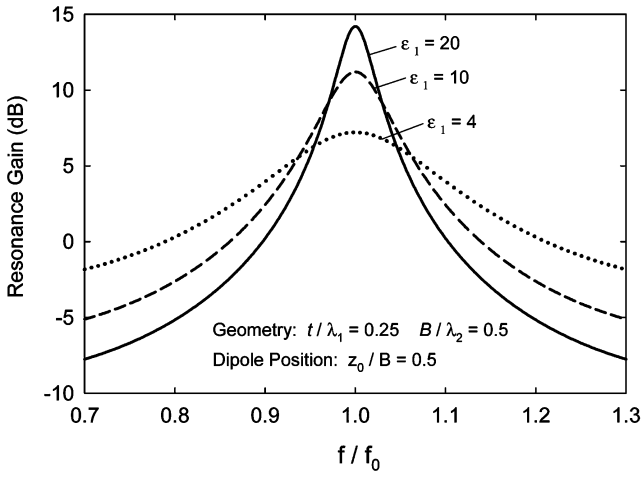

Fig. 9. Resonance gain versus frequency of superstrate-substrate geometry ($\varepsilon_2 = 2.1, \mu_1 = \mu_2 = 1$).

of the black regions show up every half-wavelength distance in both t and B, called the resonant condition since this kind of maximum voltage transfer happens when the circuit system is in resonance. The dipole should be located where voltage strength is highest. In the resonance case of $B = 0.5\lambda_2$, the antenna is located in the middle of the substrate, $z_0 = 0.5B$.

At the resonant condition, transmission line acts as a quarter wave transformer so that the impedance at $z = -H$ is noted that $Z_{\text{in}} = \infty$ and the total reflection coefficient for this case is $\Gamma_t = 1$. The high-gain curve in Fig. 6 is the geometrical relationship between the superstrate and substrate thicknesses, t and B, at high gain, obtained from the variation of maximum voltage strength in transmission-line, and includes resonant and off-resonant conditions. This high-gain curve is effective finding the highest gain with any thickness of superstrate. For

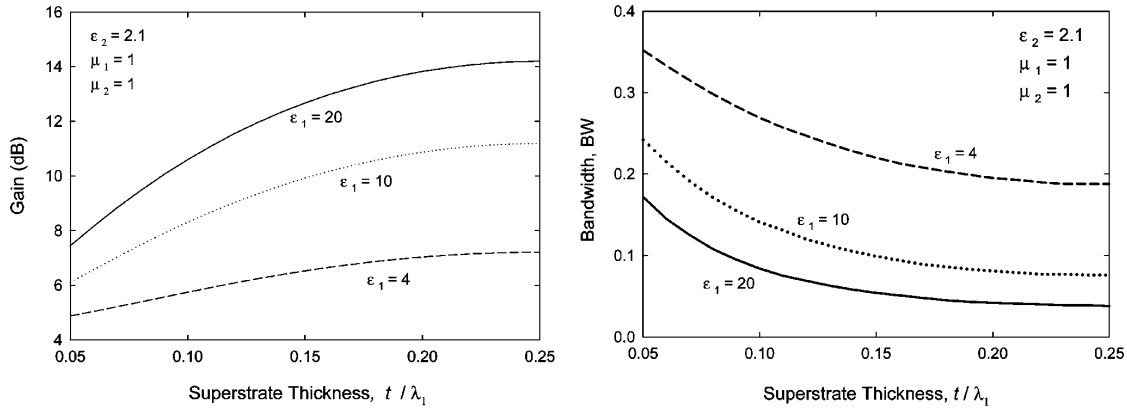

Fig. 10. Gain and bandwidth variations for high-gain condition (the geometry follows the high-gain curve for a given superstrate thickness, t) (a) Gain variation and (b) bandwidth variation.

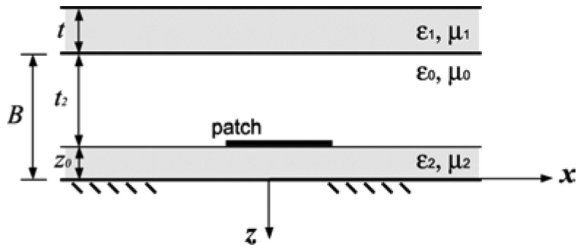

Fig. 11. Microstrip antenna covered by superstrate for experimental investigation.

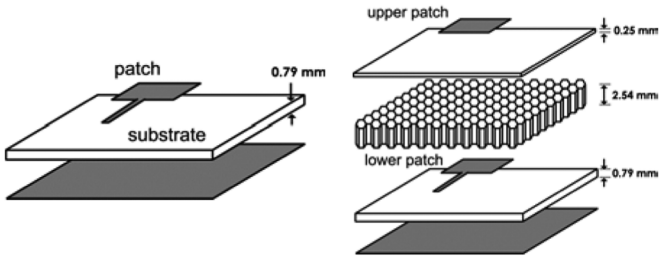

Fig. 12. Microstrip antenna for experiments (designed at 12.2 GHz) (a) MA1 (patch length: 7.7 × width: 13.4 mm). (b) MA2 (upper patch: 7.6 mm^2, lower patch: 8.0 mm^2).

example, high gain can be obtained in the substrate thickness $B > 0.5\lambda_2$ when superstrate thickness $t < 0.25\lambda_1$. Fig. 7 shows the voltage distribution in the transmission line at resonant and off-resonant conditions. The resonant circuit provides the maximum voltage transfer from the incident voltage wave to the line voltage strength.

III. Gain and Bandwidth

For the thinnest layers possible in resonant condition, it is observed that the superstrate is quarter wavelength, the bottom substrate is half-wavelength thick, and dipole is in the middle of the bottom substrate. Under the resonant condition, a very high

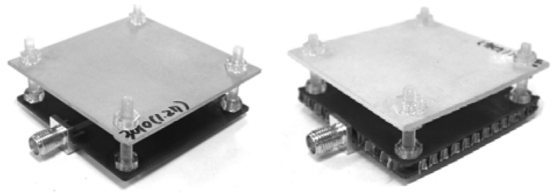

(a) MA1 with superstrate (b) MA2 with superstrate

Fig. 13. Prepared superstrate-covered antenna structure.

gain is produced with $\varepsilon_1 \gg 1$. The asymptotic formula for gain at $\theta = 0$ follows from (3) that

$$\mathrm{gain}(0,\phi) \sim \frac{|V_\theta(0)|^2}{n_2\mu_2} \tag{7}$$

where $V_\theta(0)$ is the voltage at $z = -z_0$ and can be replaced by $V_\phi(0)$ because they are the same at $\theta = 0$. Fig. 8 shows gain versus ε_1 for some different ε_2 values. Higher gain can be obtained with higher ε_1.

The bandwidth is inversely proportional to gain, which sets a limit to an achievable gain, gain bandwidth is determined here as

$$BW = \frac{f_2 - f_1}{f_0} \tag{8}$$

where f_1 and f_2 are half-power frequencies. Fig. 9 shows variations of gain with frequencies in resonant conditions. A higher ε_1 gives not only a greater gain, but also greater change in the gain away from the resonant frequency. Fig. 10 shows the gain and bandwidth variation in the high-gain condition. When the geometry is closer to resonance, the narrower bandwidth as well as the higher gain is obtained. This is the fundamental restriction. Therefore, the off-resonant condition with a thin superstrate is practically suited to a high-gain antenna in bandwidth.

TABLE I
SUPERSTRATE MATERIALS FOR EXPERIMENTS

Material	Property		Thickness (mm)
	ε_r	tanδ	
RT/duroid5880 (Rogers) Glass Fiber / PTFE	2.2	0.0009	0.79 1.58
RO3003 (Rogers) PTFE Ceramic	3	0.0013	0.76 1.52
UGN200 (SK Chemicals) Glass Fiber / Epoxy	4	0.03	1 2
RO3010 (Rogers) PTFE Ceramic	10.2	0.0035	0.64

IV. EXPERIMENTS

The theoretical model is an electric dipole embedded in the substrate with the addition of a superstrate over the substrate. For the practical application, this technique is applied to a microstrip antenna above which the superstrate is placed, as shown in Fig. 11. The substrate thickness, z_0, does not influence on the gain, therefore it can be arbitrarily determined in accordance with the design of the patch antenna [11], [12]. Thickness, position and property of a superstrate are the key design factors for the gain enhancement in practice.

Two types of microstrip antennas are prepared at the central frequency of 12.2 GHz. One is a conventional microstrip patch antenna, and the other is a stacked-patch microstrip antenna. For convenience, the microstrip antenna with one patch is named MA1 and the antenna with stacked patches is MA2. Fig. 12 shows the designed structures of MA1 and MA2. MA2 has two radiating patches that interact with each other to make dual resonances and a wide bandwidth [14], [15]. The two patches are separated by honeycomb that gives a mechanical stability as well as a free space. RT/duroid 5880 ($\varepsilon_r = 2.2, \tan\delta = 0.0009$) is used for substrates for the antennas.

Dielectric superstrates for the high-gain conditions are prepared and listed in Table I. High-gain condition is experimentally set up with the fabricated antennas and the prepared superstrates as shown in Fig. 13. The condition is found by changing the position of the superstrate layer and measuring a gain, and the position at maximum gain is recorded.

V. RESULTS AND DISCUSSION

The theoretical and experimental relationships between the thickness, t and position, B of the superstrate at the high-gain condition are presented in Fig. 14. The theoretical curves are obtained from the transmission-line analogy with $\varepsilon_2 = 1$. The experimental distance, B is slightly smaller than the theoretical results for both MA1 and MA2.

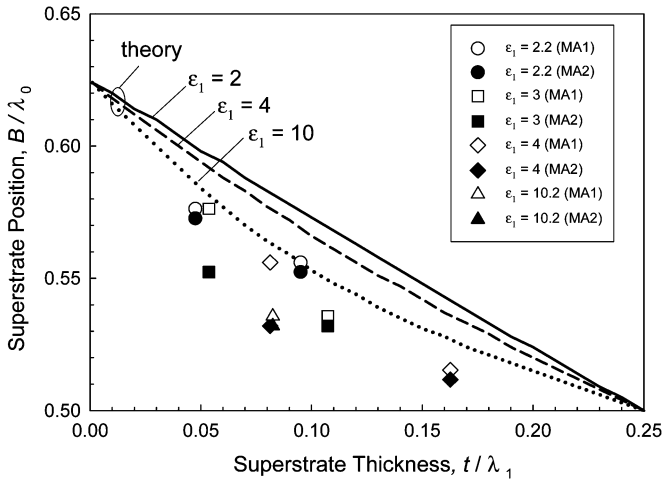

Fig. 14. Measured high-gain conditions.

Changes of resonant frequency and impedance bandwidth are investigated. Measurements are performed with a Network Analyzer 8510 under laboratory conditions. Fig. 15(a) shows results for MA1. All antennas have a shift in resonant frequency, which depends on the thickness and dielectric constant of superstrate; that is, the higher the gain, the more the resonant frequency shifts. The bandwidth also changes along the resonant frequency. It becomes narrower in antennas that experience a greater shift in resonant frequency. The impedance characteristics for MA2 are shown in Fig. 15(b). The frequency shift is much tempered by their wide bandwidth. However, the return loss more goes up as the geometry is closer to resonance. For superstrates of $\varepsilon_1 = 4$ and $t = 0.16\lambda_1$, and $\varepsilon_1 = 10.2$ and $t = 0.08\lambda_1$, the effect is so strong that the wideband effect disappears.

A frequency shift due to the existence of a superstrate above the antenna is seen. The resonant frequency of a microstrip antenna covered with a superstrate layer can be determined when the effective dielectric constant of the structure is known. The

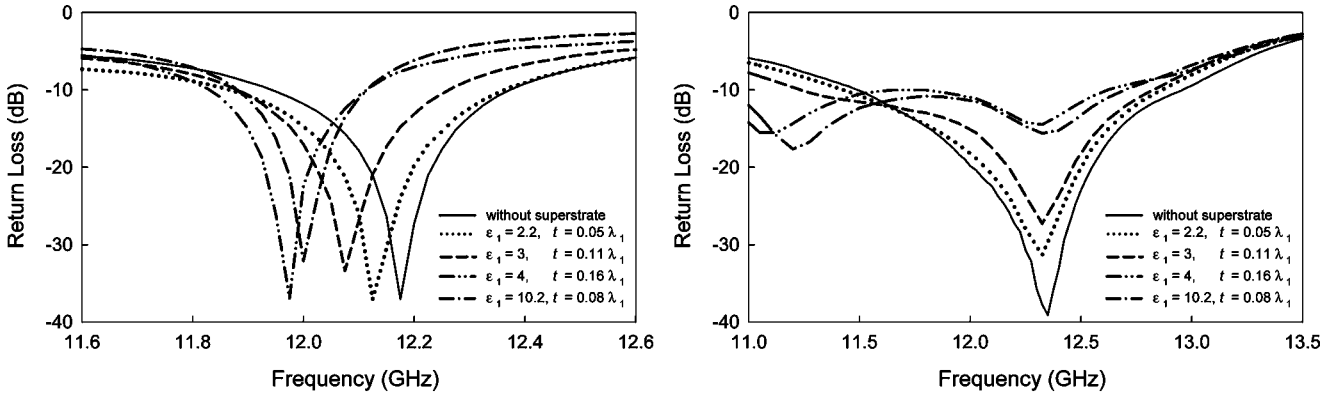

Fig. 15. Measured return losses at high-gain conditions (superstrate position, B is marked in Fig. 14 for each measurement). (a) MA1 and (b) MA2.

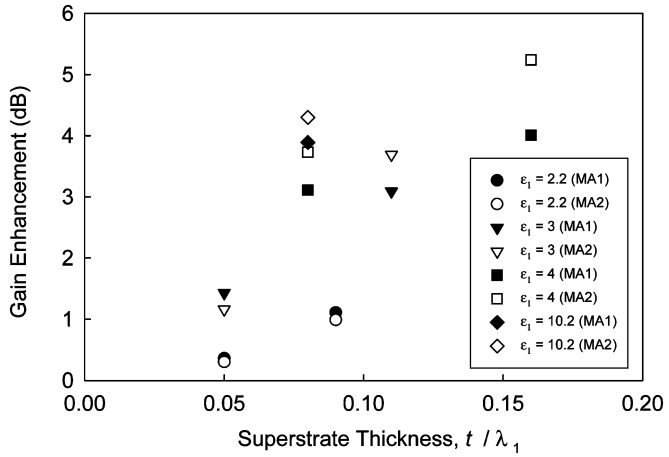

Fig. 16. Measured gain enhancement at high-gain conditions (superstrate position, B is marked in Fig. 14 for each measurement).

change in the resonant frequency relative to the case without superstrate may be expressed as [13]

$$\frac{\Delta f_r}{f_r} = \frac{\varepsilon_e - \varepsilon_{e0}}{\varepsilon_e + \varepsilon_{e0}} \tag{9}$$

with

$$\varepsilon_{e0} = \frac{\varepsilon_r + 1}{2} + \frac{\varepsilon_r - 1}{2} \frac{1}{\left(1 + 12\frac{h}{w}\right)^{1/2}} \text{ for } \frac{w}{h} \gg 1 \tag{10}$$

where ε_e and ε_{e0} are the effective dielectric constant with and without superstrate, respectively, and w is the patch width and h is the substrate thickness of dielectric constant ε_r. From (9), it is explained that greater change in resonant frequency means greater change in effective dielectric constant. The smaller experimental distance, B than in theory in Fig. 14 is also explained with the change in effective dielectric constant. It is important to determine the effect of a superstrate layer on the impedance characteristics of the antenna in order to introduce appropriate corrections in the design parameters, such as the feed position and impedance matching.

Radiation patterns are measured in an anechoic chamber. The gain of the antenna is determined by using a standard gain horn antenna (SAS-585, A. H. Systems Inc.) that is also measured in the same condition. The gain enhancements at high-gain conditions are shown in Fig. 16. The gains of MA1 and MA2 are 8.1 and 8.2 dBi, respectively. The higher gain is enhanced as the geometry is closer to resonance and the superstrate has a higher dielectric constant. The radiation patterns are presented in Fig. 17. The radiation pattern without the superstrate is superimposed; all patterns are H-plane patterns of symmetric shape to facilitate comparison. Higher gain antennas have a radiation pattern of narrower beamwidth. An explanation is that the superstrate concentrates the beam by turning the incoming spherical phase front into an outgoing plane one such as a microwave lens [16]–[19].

Antenna-integrated composite structure is designed using the high-gain condition that involves the sandwich geometry. Fig. 18 shows detailed design result. The embedded antenna is MA2 in Fig. 12(b) and the superstrate layer is glass/epoxy composites ($\varepsilon_1 = 4$ and $t = 1$ mm). For the high-gain condition, honeycomb of 10 mm thickness (t_2) is placed. Fig. 19 shows the radiation patterns of fabricated structure. It has gain 11.2 dBi at the central frequency of 12.2 GHz. Gains in bandwidth do not change significantly; they are 11.91 dBi at 11.7 GHz and 12.25 dBi at 12.75 GHz, and the radiation patterns are almost the same. By exploiting high-gain condition at off-resonance, the perfect integration is confirmed without reducing either of mechanical and electrical performances.

VI. Conclusion

The gain of an antenna can be further increased by multilayer geometry. The resonant condition is the maximum gain condition by the structural resonance, but the degradation of antenna performances, such as frequency drift and narrow impedance bandwidth is followed by the high gain in a practical application. The high-gain condition at off-resonance, which is a significant new concept, should be applied in a real design of high-gain antennas that takes the bandwidth into account. It makes it possible

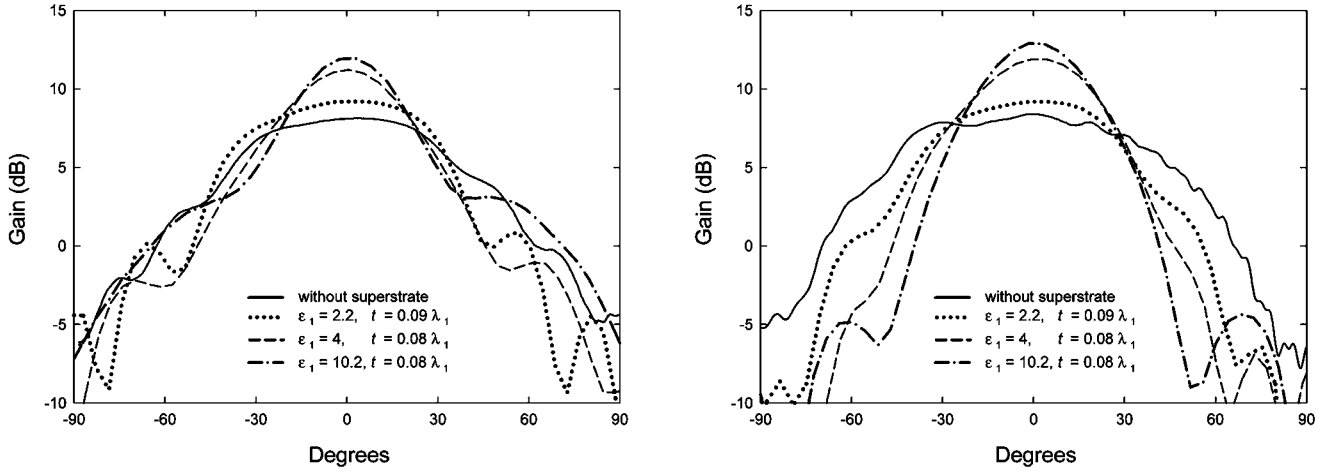

Fig. 17. Measured radiation patterns at high-gain conditions (superstrate position, B is marked in Fig. 14 for each measurement). (a) MA1 and (b) MA2.

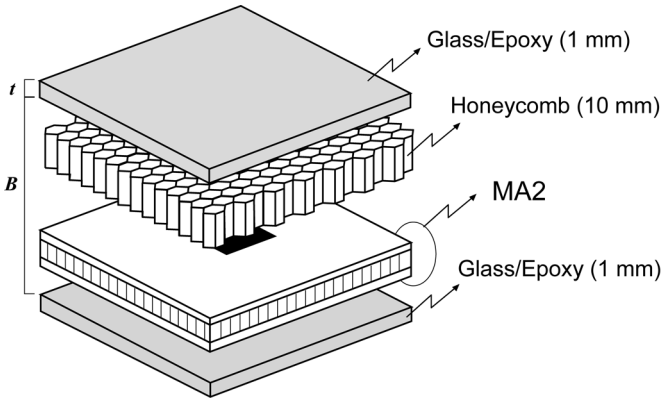

Fig. 18. Designed antenna-integrated composite structure ($\varepsilon_1 = 4$, $t = 0.08\lambda_1$, $B = 0.55\lambda_0$).

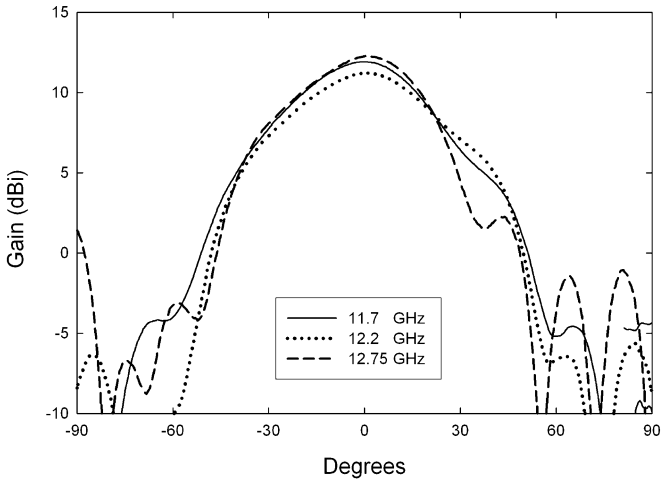

Fig. 19. Measured radiation patterns of antenna-integrated composite structure.

to use practical superstrates of moderate thickness and to insert microstrip antenna into mechanical structures with gain enhancement, indicating the perfect integration without reducing either of mechanical and electrical performances.

REFERENCES

[1] A. J. Lockyer, K. H. Alt, D. P. Coughlin, M. D. Durham, J. N. Kudva, A. C. Goetz, and J. Tuss, "Design and development of a conformal load-bearing smart-skin antenna: Overview of the AFRL smart skin structures technology demonstration (S^3TD)," *Proc. SPIE*, vol. 3674, pp. 410–424, 1999.

[2] A. J. Lockyer, J. N. Kudva, D. Kane, B. P. Hill, C. A. Martin, A. C. Goetz, and J. Tuss, "Qualitative assessment of smart skins and avionics/structures integration," *Proc. SPIE*, vol. 2189, pp. 172–183, 1994.

[3] J. Tuss, A. Lockyer, K. Alt, F. Uldirich, R. Kinslow, J. Kudva, and A. Goetz, "Conformal loadbearing antenna structure," in *Proc. 37th AIAA Structural Dynamics and Materials Conf.*, 1996, pp. 836–843, AIAA-96-1415-CP.

[4] Delphi Fuba Multiple Antenna Reception System [Online]. Available: http://www.delphi.com

[5] C. S. You and W. Hwang, "Design and fabrication of composite smart structures with high electrical and mechanical performances for future mobile communication," *Mechanics of Composite Materials*, vol. 40, no. 3, pp. 237–246, 2004.

[6] C. S. You, W. Hwang, and S. Y. Eom, "Design and fabrication of composite smart structures for communication, using structural resonance of radiated field," *Smart Materials and Structures*, vol. 14, no. 2, pp. 441–448, 2005.

[7] C. S. You and W. Hwang, "Design of load-bearing antenna structures by embedding technology of microstrip antenna in composite sandwich structure," *Composite Structures*, vol. 71, no. 3–4, pp. 378–382, 2005.

[8] N. G. Alexopoulos and D. R. Jackson, "Gain enhancement methods for printed circuit antennas," *IEEE Trans. Antennas Propagat.*, vol. AP-33, pp. 976–987, 1985.

[9] N. G. Alexopoulos and D. R. Jackson, "Fundamental superstrate (cover) effects on printed circuit antennas," *IEEE Trans. Antennas Propag.*, vol. AP-32, pp. 807–816, 1984.

[10] X. Shen, G. Vandenbosch, and A. Van de Capelle, "Study of gain enhancement method for microstrip antennas using moment method," *IEEE Trans. Antennas Propag.*, vol. 43, pp. 227–231, 1995.

[11] X. Shen, P. Delmotte, and G. Vandenbosch, "Effect of superstrate on radiated field of probe fed microstrip patch antenna," in *Proc. Inst. Elect. Eng.-Microw. Antennas Propag.*, 2001, vol. 148, pp. 141–146.

[12] H. Y. Yang and N. G. Alexopoulos, "Gain enhancement methods for printed circuit antennas through multiple substrates," *IEEE Trans. Antennas Propag.*, vol. AP-35, pp. 860–863, 1987.

[13] I. J. Bahl, P. Bhartia, and S. S. Stuchly, "Design of microstrip antennas covered with a dielectric layer," *IEEE Trans. Antennas Propag.*, vol. AP-30, pp. 314–318, 1982.

[14] Q. Lee, K. F. Lee, and J. Bobinchak, "Characteristics of a two-layer electromagnetically coupled rectangular patch antenna," *Electron. Lett.*, vol. 23, no. 20, pp. 1070–1072, 1987.

[15] R. Q. Lee and K. F. Lee, "Effects of parasitic patch sizes on multi-layer electromagnetically coupled patch antenna," *Proc. IEEE Int. Symp. Antennas and Propagation Society*, vol. 2, pp. 624–627, 1989.

[16] X. Shen and G. Vandenbosch, "Aperture field analysis of gain enhancement method for microstrip antennas," in *Proc. 10th Int. Conf. on Antennas and Propagation*, 1997, vol. 1, pp. 186–189.
[17] C. Morrow, P. Taylor, and H. Ward, "Phase and amplitude measurements in the near field of microwave lenses," *IRE Int. Convention Record*, vol. 6, pt. 1, pp. 166–176, 1958.
[18] D. N. Black and J. C. Wiltse, "Millimeter-wave characteristics of phase-correcting Fresnel zone plates," *IEEE Trans. MTT*, vol. 35, no. 12, pp. 1122–1129, 1987.
[19] H. D. Hristov and M. H. A. J. Herben, "Millimeter-wave Fresnel zone planar lens and antenna," *IEEE MTT-S IMS Digest*, vol. 2, pp. 553–556, 1995.

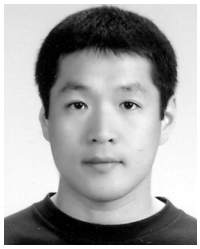

Chisang You received the B.S. degree in mechanical engineering from Sogang University, Seoul, Korea, in 1999, and the Ph.D. degree in mechanical engineering from Pohang University of Science and Technology (Postech), Pohang, Korea, in 2004.

He is currently a Postdoctoral Researcher in the School of Electrical and Computer Engineering, Georgia Institute of Technology (Georgia Tech), Atlanta. The areas in which he is very much interested are RF-integrated mechanical structures including antennas and composite structures, and RFMEMS.

Manos M. Tentzeris (S'89–M'98–SM'03) received the diploma degree in electrical and computer engineering (*magna cum laude*) from the National Technical University of Athens, Greece, and the M.S. and Ph.D. degrees in electrical engineering and computer science from the University of Michigan, Ann Arbor.

He was a Visiting Professor with the Technical University of Munich, Germany for summer 2002, where he introduced a course in the area of high-frequency packaging. He is currently an Associate Professor with the School of Electrical and Computer Engineering, Georgia Institute of Technology (Georgia Tech), Atlanta. He is the Georgia Tech NSF-Packaging Research Center Associate Director for RF Research and the RF Alliance Leader. He is also the leader of the RFID Research Group of the Georgia Electronic Design Center (GEDC) of the State of Georgia. He has given more than 40 invited talks in the same area to various universities and companies in Europe, Asia and America. He has published more than 200 papers in refereed Journals and Conference Proceedings and eight book chapters and he is in the process of writing two books.

Dr. Tentzeris is a member of the International Scientific Radio Union (URSI) Commission D, an Associate Member of EuMA, and a member of the Technical Chamber of Greece. He was a recipient of the 1997 Best Paper Award of the International Hybrid Microelectronics and Packaging Society for the development of design rules for low-crosstalk finite-ground embedded transmission lines. He received the 2000 NSF CAREER Award for his work on the development of MRTD technique that allows for the system-level simulation of RF integrated modules, the 2001 ACES Conference Best Paper Award, the 2002 International Conference on Microwave and Millimeter-Wave Technology Best Paper Award (Beijing, China) for his work on Compact/SOP-integrated RF components for low-cost high-performance wireless front-ends, the 2002 Georgia Tech-ECE Outstanding Junior Faculty Award, the 2003 NASA Godfrey "Art" Anzic Collaborative Distinguished Publication Award for his activities in the area of finite-ground low-loss low-crosstalk coplanar waveguides, the 2003 IBC International Educator of the Year Award, the 2003 IEEE CPMT Outstanding Young Engineer Award for his work on 3-D multilayer integrated RF modules, and the 2004 IEEE Transactions on Advanced Packaging Commendable Paper Award. He was also the 1999 Technical Program Co-Chair of the 54th ARFTG Conference, Atlanta, GA and he is the Vice-Chair of the RF Technical Committee (TC16) of the IEEE CPMT Society. He has organized various sessions and workshops on RF/Wireless Packaging and Integration in IEEE ECTC, IMS, and APS Symposia in all of which he is a member of the Technical Program Committee in the area of "Components and RF." He is an Associate Editor of the IEEE TRANSACTIONS ON ADVANCED PACKAGING.

Woonbong Hwang received the B.S. degree in precision mechanical engineering from Hanyang University, Seoul, Korea, in 1982 and the M.S. and Ph.D. degrees in mechanical engineering from SUNY at Buffalo, Buffalo, NY, in 1985 and 1988, respectively.

In 1988, he joined the Department of Mechanical Engineering at Pohang University of Science and Technology (Postech), Korea, where he is currently a Full Professor and heads the NSCS Research Group. From 2000 to 2001, he was a Visiting Scholar at the Digital Appliance Research Lab. in LG Electronics Inc. Since 2002, he has helped develop academic programs in creative engineering including axiomatic design and TRIZ. He has published more than 120 papers in internationally renowned journals and conference proceedings. His research interests include composite materials, nanomechanics with nanosized honeycomb, and RF-integrated mechanical structures.